Multiple Factors Influence Glomerular Albumin Permeability in Rats

Ruben M. Sandoval, Mark C. Wagner, Monica Patel, Silvia B. Campos-Bilderback, George J. Rhodes, Exing Wang, Sarah E. Wean, Sherry S. Clendenon, and Bruce A. Molitoris

Division of Nephrology, Department of Medicine, and the Indiana Center for Biological Microscopy, Indiana University School of Medicine and the Richard L. Roudebush Veterans Affairs Medical Center, Indianapolis, Indiana

ABSTRACT

Different laboratories recently reported incongruous results describing the quantification of albumin filtration using two-photon microscopy. We investigated the factors that influence the glomerular sieving coefficient for albumin (GSC_A) in an effort to explain these discordant reports and to develop standard operating procedures for determining GSC_A. Multiple factors influenced GSC_A, including the kidney depth of image acquisition (10–20 μm was appropriate), the selection of fluorophore (probes emitting longer wavelengths were superior), the selection of plasma regions for fluorescence measurements, the size and molecular dispersion characteristics of dextran polymers if used, dietary status, and the genetic strain of rat. Fasting reduced the GSC_A in Simonsen Munich Wistar rats from 0.035 ± 0.005 to 0.016 ± 0.004 ($P < 0.01$). Frömter Munich Wistar rats had a much lower GSC_A in both the fed and the fasted states. Finally, we documented extensive albumin transcytosis with vesicular and tubular delivery to and fusion with the basolateral membrane in S1 proximal tubule cells. In summary, these results help explain the previously conflicting microscopy and micropuncture data describing albumin filtration and highlight the dynamic nature of glomerular albumin permeability.

J Am Soc Nephrol 23: 447–457, 2012. doi: 10.1681/ASN.2011070666

Over the past several years, the roles the glomerular filtration barrier and the proximal tubule play in the development of albuminuria have been debated.[1,2] The present textbook model, in which albumin filtration across a normal glomerulus is thought to be minimal, has recently been challenged. A wide array of genetic, molecular, biochemical, and imaging studies are consistent with proximal tubule cells (PTCs) having a role in reclaiming filtered proteins, including albumin, and thus minimizing proteinuria. These studies include the following: knockout mice lacking Na+–H+ exchanger isoform 3 or chloride channel-5;[3] megalin-cubilin complex defects;[4] Rab 38–mediated tubular proteinuria and albuminuria;[5] statin-mediated inhibition of guanosine triphosphatase prenylation with reduced proximal tubule (PT) endocytosis;[4,6–8] mice lacking FcRn, the IgG and albumin receptor;[9,10] and selective PTC injury using D-serine[11] or the selective expression of diphtheria toxin receptor on PTC.[12] In a preliminary communication, Menzel and colleagues showed that PT reabsorption and transcytosis of podocyte produced and secreted albumin labeled with V5 and hemagglutinin tags.[13] Finally, recently published data[14] using advanced scanning electron microscope imaging techniques indicate that the podocyte slit diaphragm has pores that are much larger than previously determined and are of the size required for albumin filtration.

The development of *in vivo* two-photon microscopy has enabled the direct visualization and quantitation of fluorescent compounds as they filter through the glomerulus and are endocytosed by

Received July 8, 2011. Accepted October 21, 2011.

Published online ahead of print. Publication date available at www.jasn.org.

Correspondence: Dr. Bruce A. Molitoris, Indiana University School of Medicine, Bld R2-E251, 950 West Walnut Street, Indianapolis, IN 46202. Email: bmolitor@iupui.edu

proximal tubule cells.[15,16] Direct visualization of intracellular trafficking, catabolism, and the reclamation of filtered proteins by the PT has enabled albumin filtration and reabsorption to be observed and quantified.[17] We have previously used this technique to determine the glomerular sieving coefficient for albumin (GSC_A) in Simonsen Munich Wistar (SMW) rats under physiologic fed conditions and reported a GSC_A of 0.035,[18,19] a number higher than reported with micropuncture studies in Sprague-Dawley or Frömter Munich Wistar (FMW) rats.[2,20–22] Because this value does not agree with previous micropuncture data and has been disputed by others using two-photon approaches,[23–26] we have undertaken extensive studies to further characterize this discrepancy, including the effects of methods on the detection and quantification of fluorescent molecules within the kidney. The present data substantiate our previous results; provide optimal study parameters; and explain that differences in GSC_A reported in the literature result from the different technical approaches, genetic strains, nutritional conditions, and fluorescent probes used in the studies. Our new findings also indicate the GSC_A is not static but dynamic, changing dramatically depending on nutritional circumstances.

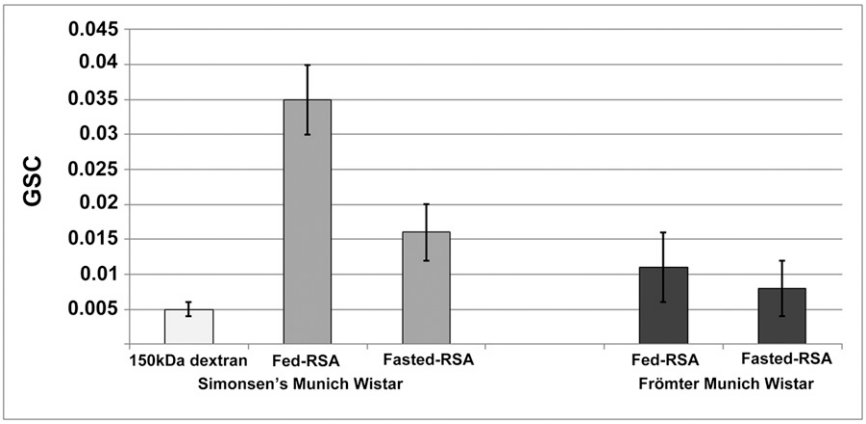

Figure 1. SMW rats filter higher levels of albumin than FMW rats. In SMW rats, dietary fasting reduced GSC_A values from 0.035±0.005 to 0.016±0.004 (n=9 glomeruli; three rats each; $P<0.01$). In their normal fed state, the FMW strain at 8 weeks of age had a GSC_A value three times lower (0.010±0.001) and a fasting GSC_A of 0.008±0.004 (n=24 glomeruli; 4 rats for fed; n=14 glomeruli; 3 rats for fasting; $P<0.05$). To investigate whether the higher GSC values for albumin obtained in this and previous studies using the SMW strain were not a result of out-of-focus fluorescence within Bowman's space, a 150-kD fluorescein dextran was examined and found to generate a GSC value of 0.005±0.001.

RESULTS

Glomerular Albumin Permeability Depends on Dietary Status and Genetics

Major differences in the nutritional state of the rat and type of MW rat studied exist between our previously reported data on two-photon GSC_A and micropuncture. Micropuncture data have been generated using FMW rats in the fasting condition, whereas we used SMW rats in the fed condition.[18,19] Because feeding status increases urinary albumin and prostprandial GFR has previously been quantified in rats,[27] we first set out to determine the effects of feeding on GSC_A. As shown in Figure 1, after an overnight fast SMW rats showed a marked reduction in GSC_A: from 0.035±0.005 to 0.016±0.004 (mean ± SD; $P<0.01$). The determinants for this change are yet to be investigated, but the magnitude was striking and indicates that feeding has a dramatic effect on GSC_A.

FMW rats are used by investigators performing micropuncture studies[2,20,22] because they have more surface glomeruli than do SMW rats and the males spontaneously develop focal glomerular sclerosis and progressive proteinuria/albuminuria with increasing age.[28] Therefore, we wanted to directly compare two-photon with previous micropuncture-measured GSC_A data in the same strain of MW rats and determine the effect of fasting. Male FMW rats younger than 10 weeks of age had a GSC_A of 0.010±0.001 under fed conditions and a GSC_A of 0.007±0.001 under fasting conditions ($P<0.05$). Twenty-four-hour urinary albumin at 6 weeks of age was 72±35 mg (n=4 rats). These data show considerable differences in GSC_A for FMW and SMW rats and a marked effect of fed and fasting status in both strains.

Characterizing Appropriate Parameters for Determining Two-Photon GSCs: Measuring at Superficial Tissue Depths Increases Accuracy

To make sure our study parameters allowed for maximal determination and quantification of GSC_A, we characterized the variables involved with use of two-photon techniques to determine glomerular permeability, because attenuation of fluorescence occurs for all probes at increasing depths of tissue observation as a result of photon scatter and absorption.[29,30] The magnitude of this decrease depends on the spectral properties of each probe and the tissue under study. Therefore, we first examined the effect of tissue depth on fluorescent probe intensity for two common fluorophores with different emission wavelengths. In Figure 2A, an image taken at tissue depth of 12 μm shows a characteristic yellow color in the capillary loops and surrounding vasculature due to the combination of red and green fluorescent emissions being detected with nearly equal intensity. In Figure 2B, at a depth of 28 μm, a greater loss of green fluorescent emissions resulted in a color shift from yellow to red-orange within the capillary loops. An orthogonal view in Figure 2C reveals in detail the more rapid deterioration in green fluorescent signal over depth as the vascular plasma color becomes predominantly red with increasing depth. A graph quantifying the fall-off in fluorescent intensity with tissue

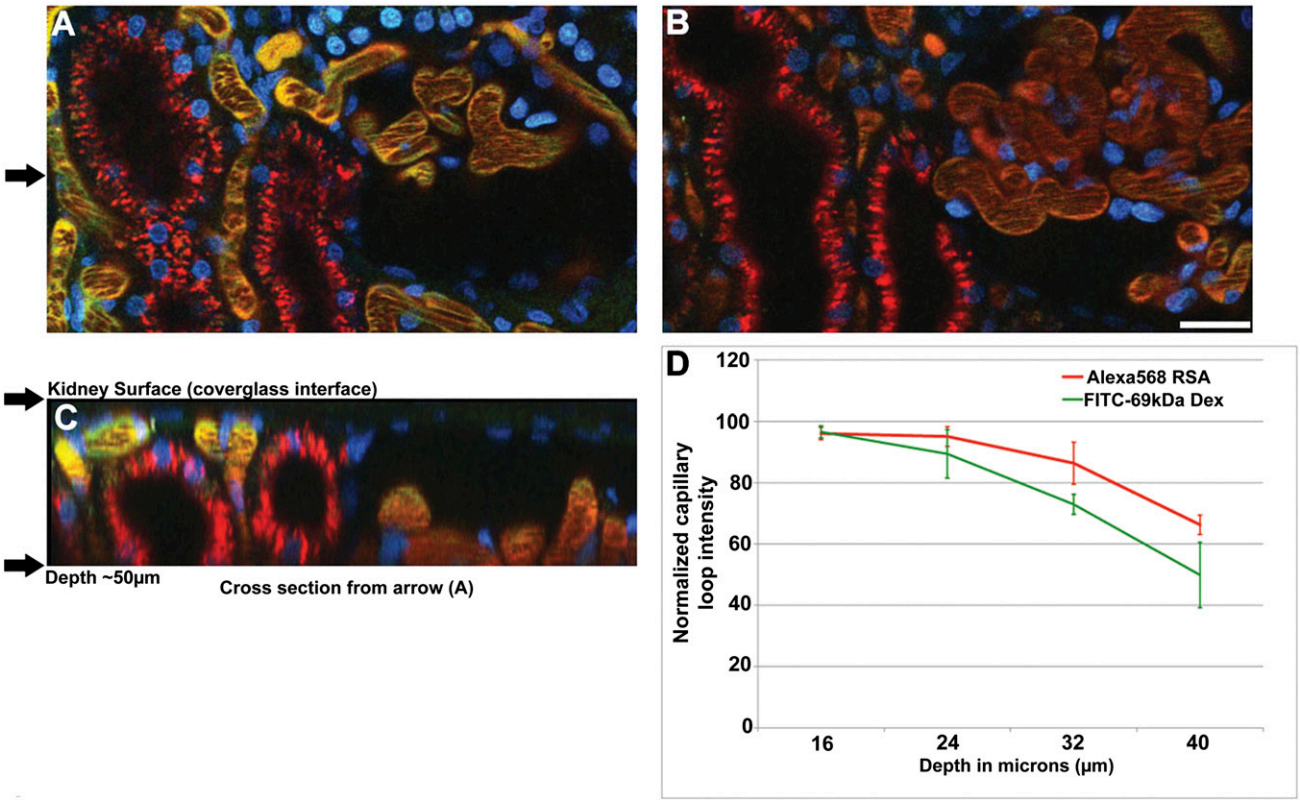

Figure 2. Emitted light from shorter-wavelength fluorophores is more susceptible to scatter at deeper tissue depths. Plasma intensities from a fluorescein 69.7-kD dextran (with a peak emission of 525 nm) and Alexa 568-RSA (with a peak emission of 603 nm) within a three-dimensional glomerular volume were quantified. (A) A mixture of the two probes (green and red) appeared yellow within superficial capillary loops (approximately 12 μm into the glomerular volume) indicating a nearly equal emission for both probes. (B) At a depth of approximately 28 μm within the same glomerulus, a color shift from yellow to orange-red occurred as the contribution of green fluorescence emission within the focal plane was reduced compared with the longer-emitting red probe. (C) An orthogonal X-Z projection taken at a reference point in (A) (arrow) shows a more gradual reduction in green fluorescence through the image. (D) Intensity values confirm the more rapid plasma intensity decay of the green fluorescein 69-kD dextran. Normalized intensity values of 96%±2% for both probes were seen at depths of 16 μm. However, at 40 μm the normalized values were 66.3%±3.1% for the Alexa 568-RSA probe and 49.8%±10.6% for fluorescein ($P<0.01$) ($n=3$ glomeruli; 4 capillary loop segments/focal plane). (Bar=25 μm.)

depth is shown in Figure 2D. Intensity values for fluorescein, compared with Alexa 568, decreased more rapidly with increasing depth. Because decreasing intensity reduces the ability to accurately quantify fluorescence, use of longer wavelength–emitting fluorophores is preferred, especially at increased depths.

Increasing tissue depth increased GSC_A values and variability, as shown in Supplemental Figure 1, thus reducing the reliability of the data obtained. Taken together these data indicate that the best depth and fluorophore for determination of GSCs were 10–20 μm and red-emitting fluorophores, respectively, as previously published.[18,19,31]

Enhanced Sensitivity Is Crucial in Detecting the Low Albumin Levels Present in Bowman's Space

To determine the effect of detector sensitivity on quantifying low fluorescence intensity at different tissue depths, fixed vibratome-sectioned kidney tissue was stained with a fluorescein-conjugated lectin from *Lens culinaris* and identical, sequential three-dimensional data sets were collected with different detector types and quantified. Detector type made little difference in image quality at superficial depths because very superficial depths (Figure 3A, 5-μm depth) had identical shapes among the three different detector types. However, sensitivity differed among the three types of detectors. Internal descanned multialkaline detectors showed limited sensitivity. Sensitivity was improved for the external nondescanned multialkaline detectors and was maximal with the highly sensitive gallium arsenide phosphide (GaAsP) external nondescanned detectors. The latter detectors required only half the laser power to obtain identical intensity within the same bright structure (Figure 3A) and are therefore twice as sensitive for a given excitation power. Intensity differences became even more visually apparent 10 μm deeper into the tissue, with a marked decrease in detection of lower-intensity regions with the internal detector when compared with the two external detectors (highlighted region, 15-μm depth). These data indicate that it is critical to understand detector limitations and, for any detector type, to acquire images at more superficial depths for best quantitative results.

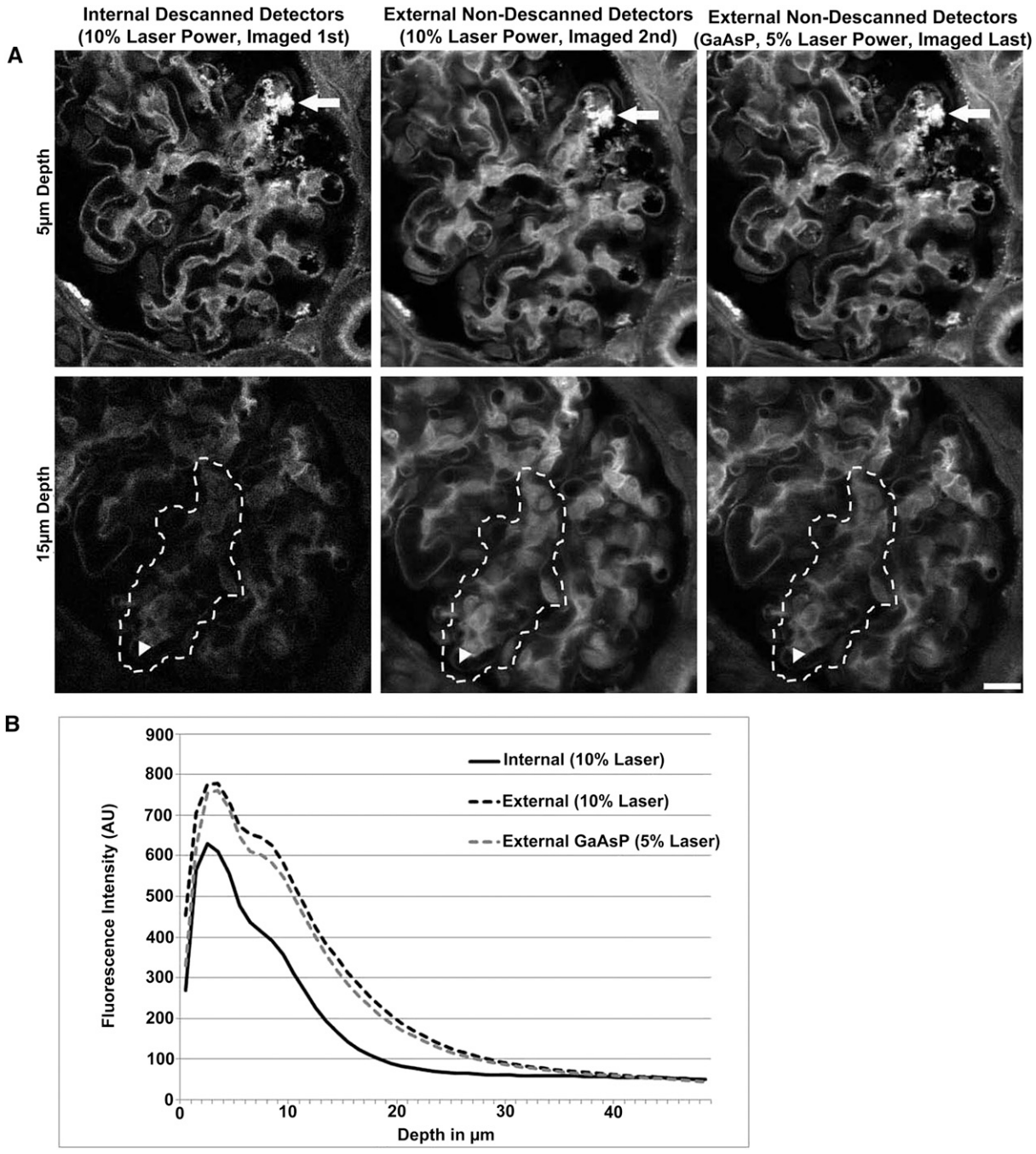

Figure 3. Internal descanned detectors have reduced photo-sensitivity at all tissue depths when compared with external nondescanned detectors. (A) Images from a perfused fixed rat kidney sectioned and stained with a fluorescein lectin. Identical three-dimensional data sets of the same glomerulus were sequentially acquired, first using internal descanned multialkaline detectors, then by external nondescanned multialkaline detectors, and finally by a highly sensitive external nondescanned GaAsP detector. In the upper three panels, at a focal depth of approximately 5 μm, image quality is similar among the three detectors. Note that the structure in the upper right (arrow) has nearly saturated intensity values, indicating the full use of dynamic range among the three detector types. Approximately 10 μm farther into the tissue section, a noticeable decrease in image quality and a marked decrease in sensitivity to corresponding dimmer structures (highlighted region) were seen between the internal descanned and the two external nondescanned detectors in the three center panels. (B) The average intensity for each focal plane obtained using the different detectors graphed as a function of depth. At nearly all depths the internal descanned detector has reduced sensitivity. At depths greater than 10 μm, this reduction in sensitivity of the internal descanned detectors is more evident, as seen by the shape of the curve. Here, a plateau occurred at more superficial depths, with the internal detector indicative of an inability to acquire and discriminate low intensity values. (Bar=15 μm.)

Detection of Plasma Fluorescence: Effect of Red Blood Cell Crowding on Quantifying Plasma Fluorescence

The inability to accurately quantify plasma fluorescence intensity due to dense red blood cell effects was cited in two invited reviews[23,25] as a mechanism for producing elevated GSCs, as we previously reported.[18,19,31] However, to our knowledge this has never been evaluated in a systematic fashion. To directly evaluate this possibility, we compared our standard acquisition method with the suggested gold standard of line scan method. Figure 4, A through D, shows a direct comparison of fluorescence intensity values from both methods. The histogram in Figure 4D shows a nearly identical overlap of cumulative intensity values for quantifying the fluorescent profile of the region highlighted in Figure 4B or the corresponding line scan in Figure 4C. These data indicate that plasma intensity values vary widely and that careful selection of the brightest values is essential, but both techniques gave similar values.

Dispersion of Dextran Polymer Size Results in Time-Dependent GSC Values

Previous investigators used dextrans in an attempt to estimate GSC_A with two-photon technology.[23,25] Commercial fluorescent dextrans come in many molecular weights, but the dispersion of molecular weights around the mean within a product has not been reported. Therefore, we carefully compared the commercially available 70-kD dextran used in previous studies[23,25] with the 69-kD dextran used in our study.[18] Figure 5A shows that the commercially available 70-kD rhodamine B dextran produced GSC values that decreased from 0.11±0.000 at 30 seconds to 0.015±0.000 45 minutes after infusion, a change spanning nearly an order of magnitude. This large delta implies a broad size dispersion of the dextrans around an average molecular weight and is consistent with accumulation of probe in the distal tubule (shown in Figure 5B) resulting from low-molecular-weight components being rapidly filtered.

The 69.7-kD dextran we used had an average GSC value of 0.048±0.008 initially and 0.019±0.002 at 24 minutes and remained stable thereafter (Figure 5A). This finding is consistent with a compound having a narrower, but not completely uniform, size distribution. Conversely, Texas Red rat serum albumin (TR-RSA) showed the least variation between the time points studied; it had a GSC of 0.027±0.009 at 30 seconds and a final value of 0.028±0.002 at 24 minutes. These TR-RSA data are consistent with those reported in similar studies for fluorescent albumin, in which individual glomeruli were followed for 90 minutes.[31]

Because polydispersion of dextrans has important implications with regard to the interpretation of GSC data, we confirmed

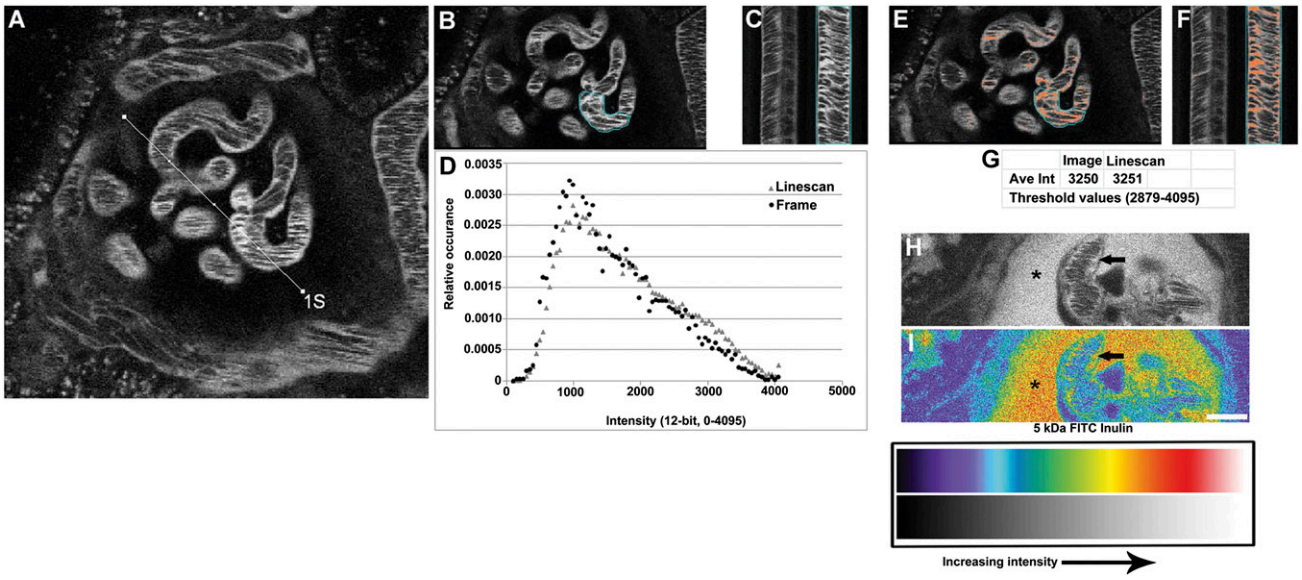

Figure 4. Red blood cells do not affect the ability to accurately detect plasma fluorescence levels. (A) Image of a glomerulus infused with a 150-kD rhodamine dextran; the line corresponds to the line scan location through the capillary loops and Bowman's space. The line scan images are shown in (C and F). The histogram shown in (D) was generated by selecting regions from frames of a movie (B) and line scan (C) and graphing the relative occurrence of all the intensity values within the selected regions. Note that this results in nearly identical overlap between both methods. Selecting the plasma fluorescence by thresholding either regions of the capillary loop (E) or the line scan (F) also gave nearly identical intensities. (G) shows the average intensity values of the image (from E) and the line scan (from F) to be 3250 and 3251, respectively. (H and I) Glomeruli from SMW rats given a constant infusion of a freely filtered FITC inulin. Note that the plasma intensities within the capillary loops (arrows) appear identical to those seen in Bowman's space (asterisks) shown in both black and white and pseudocolor. Calculation of the GSC value for FITC inulin confirmed the similar appearance with a GSC of 1.050±0.028. Underestimation of the plasma fluorescence, as predicted previously,[23,25] would have resulted in GSC values for inulin ranging up to 17.5 (if our values of 0.035 were indeed 0.002; a 17.5-fold difference). (Bar=20 μm; pseudocolor scale denotes matching grayscale values.)

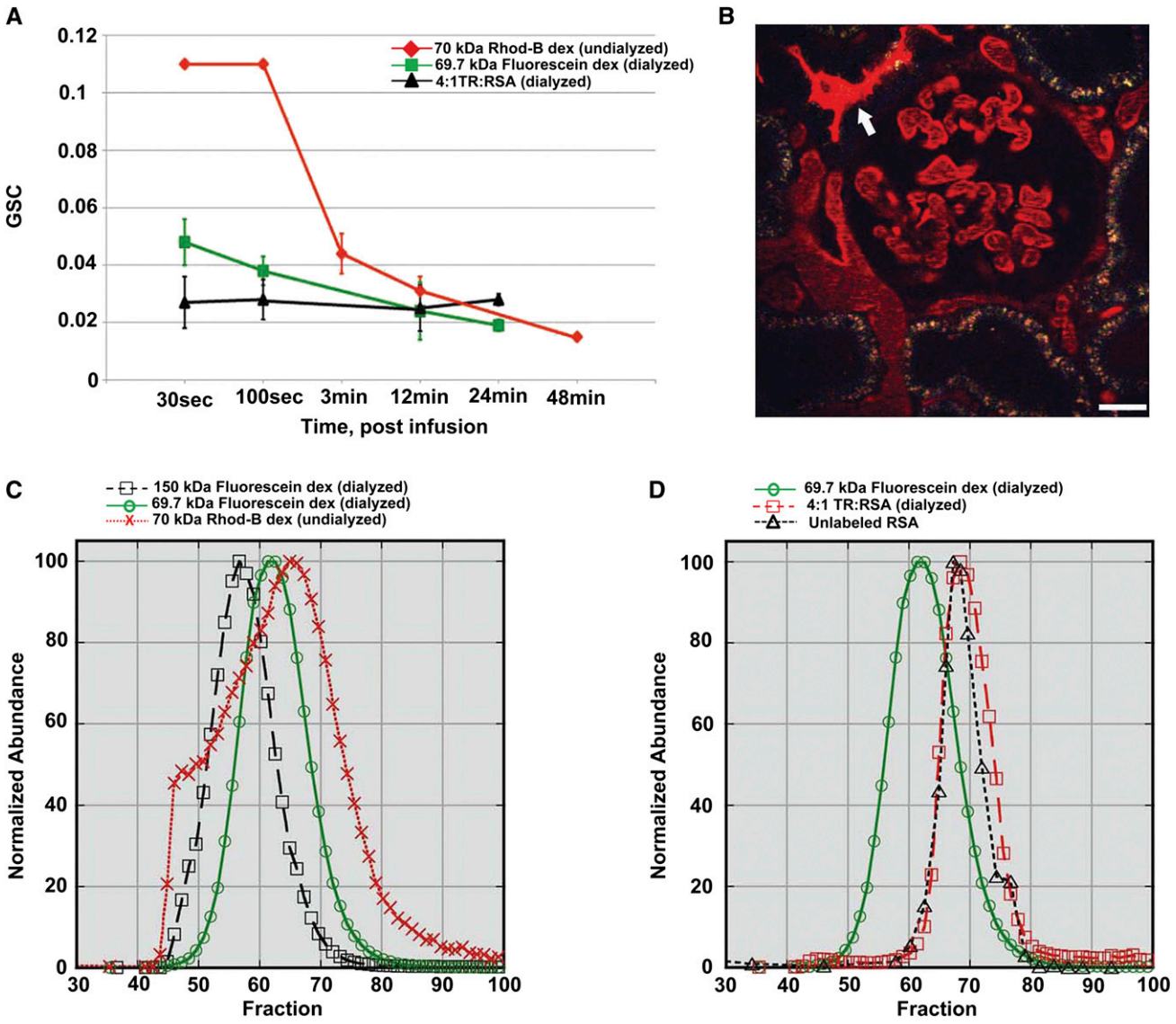

Figure 5. Fluorescent dextrans containing polymers with broadly dispersed sizes generate time-dependent GSC values. (A) SMW rats were infused with the 69.7-kD fluorescein dextran, the 70-kD rhodamine B dextran, or TR-RSA, and GSC values were calculated over time. The 70-kD rhodamine B dextran produced the greatest variance in GSC over time, with values ranging from 0.11 approximately 30 seconds after infusion to 0.015 after 45 minutes (n=2 rats; one glomeruli each/time point). The 69.7-kD fluorescein dextran initially gave a GSC value of 0.048±0.008 before settling at a value of 0.019±0.002 at 24 minutes after infusion (n=3 rats; one glomeruli each/time point). The TR-RSA gave the most consistent values throughout the time course, generating a value of 0.027±0.009 at 30 seconds after infusion and a final value of 0.028±0.002 at 24 minutes after infusion (n=3 rats; one glomeruli each/time point). (B) A micrograph of the 70-kD rhodamine B dextran with lower-molecular-weight components that have been filtered, not reabsorbed, and subsequently accumulated in a distal tubule (arrow). (C) A graph of the dispersion characteristics for a 150-kD FITC dextran, a 69.7-kD FITC dextran, and a 70-kD rhodamine B dextran using gel filtration. The 150-kD and 69.7-kD dextrans (shown in green and black tracings) had narrower elution profiles from the gel filtration column (present in fewer fractions), indicating that these compounds contained polymers more uniform in size. The 70-kD rhodamine B dextran had a much wider elution profile, indicating a sample that has a large size dispersion and contains polymers much smaller than the 70 kD eluting in higher numbered fractions to polymers larger than those found in the 150-kD fluorescein dextran sample. (D) A tracing shows the dispersion characteristics of the 69.7-kD fluorescein dextran (in green), TR-RSA (in red), and native RSA (in black). The conjugation of RSA to four TR fluorophores imparts no alteration in the size characteristic of TR-RSA because this compound and the native form have elution profiles that are narrow and virtually identical. (Bar=20 μm.)

the infusion data interpretation by directly evaluating size uniformity of the infused dextrans and TR-RSA using a gel filtration column. Both the 69.7-kD and 150-kD fluorescein dextrans had a narrow size distribution of the constituent polymers compared with the 70-kD rhodamine B dextran (Figure 5C). The 70-kD dextran contained polymers that ranged from extremely small dextrans (found at the higher-numbered fractions) to those that were larger than the 150-kD dextran (at the lower-numbered fractions). Both native RSA and TR-RSA produced identical peaks and tracings with narrower size distributions (Figure 5D). Taken together, these studies indicate that it is best to use a uniform protein to directly determine GSC and not rely on surrogate dextrans, particularly if constituent polymers are broadly dispersed.

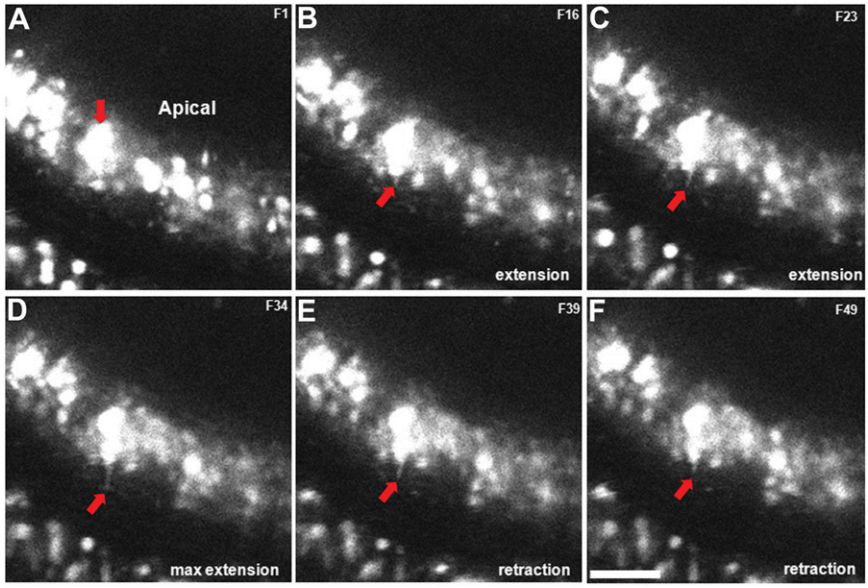

Figure 6. Transcytosis of labeled RSA occurs via tubular and vesicular structures emanating from sequestered intracellular compartments. A two-photon intravital time series taken in a SMW rat given 2 mg of Alexa 568-RSA intravenously 24 hours before imaging shows formation, extension, and retraction of a tubular structure over 50 seconds (A–F). (A) A single frame with a large accumulation of albumin (arrow; note the orientation of the apical membrane; frame 1). (B–D) The formation of a tubular structure extending from an intracellular compartment toward the basal pole of the PTC (frames 16, 23, and 34, respectively). (D) Contact is made with the basal membrane, and a lateral perpendicular spreading of fluorescence is seen along the surface of the cell (arrow; frame 34). (E and F) The tubule is retracted toward the parent structure (frames 39 and 49, respectively). In Supplemental Movie 1, more vesicles and tubular structures can be seen mediating movement of labeled albumin from intracellular pools across the basolateral membrane. (Bar=10 μm in F.)

Transcytosis of Albumin by PTCs

Because SMW rats have higher albumin permeability across the glomerulus and are not albuminuric, we postulated that they must possess a rapid method for PT albumin reabsorption and reclamation. Our previous studies have documented rapidly occurring and extensive PT reabsorption in two-photon studies and transcytosis with electron microscopy.[19] To directly determine whether transcytosis of albumin occurred intravitally, we first loaded rats with our standard dose of fluorescent albumin and then used two-photon microscopy to visualize a time series of images with a focal plane depth of approximately 1 μm for evaluation of albumin transcytosis. Figure 6 and Supplemental Movie 1 both show tubular and vesicular structures, loaded with fluorescent albumin, moved to and united with the basolateral membrane and resulting in transcytosis of reabsorbed albumin. To provide a more extensive and semi-quantitative view of this process, a single two-photon plane across a functioning PT is shown in Figure 7, along with nine inset images of individual transcytotic events occurring in different PT cells. Many more such events can be seen in Supplemental Movie 1, emphasizing the quantitative significance of this process. These data confirm and extend our previous electron microscopy immunogold documentation of albumin transcytosis.[19]

DISCUSSION

Although the clinical relevance of proteinuria (especially albuminuria) has been well documented,[32] the quantitative and mechanistic role of each "barrier" component, including the proximal tubule, in albuminuria remains an area of considerable excitement and debate.[31,33–35] Over the past 5 years, the long-standing controversy regarding the quantitative role of the proximal tubule in the development of albuminuria has reached new heights, with supporting evidence coming from many different genetic, molecular, and technical approaches.

The use of two-photon microscopy offers a unique approach to improving the understanding of the roles of glomerular filtration barrier and PT in albumin filtration and reabsorption. It allows for direct visualization and quantification of the glomerular filtration and its associated S1 PT segment in MW rats with surface glomeruli. It also permits quantification and relating of changes in structure and function longitudinally over the course of a disease process within the same glomerulus, and the corresponding S1 PT segment.

In this study, optical variables that are known to affect sensitivity and specificity in tissue were delineated for the kidney. Depth, fluorophore selection, and detector sensitivity affected the ability to correctly quantify glomerular albumin permeability. The results indicated that the appropriate depth is 10–20 μm, that longer–wavelength emitters (such as rhodamine derivatives) offered superior detection, and that using

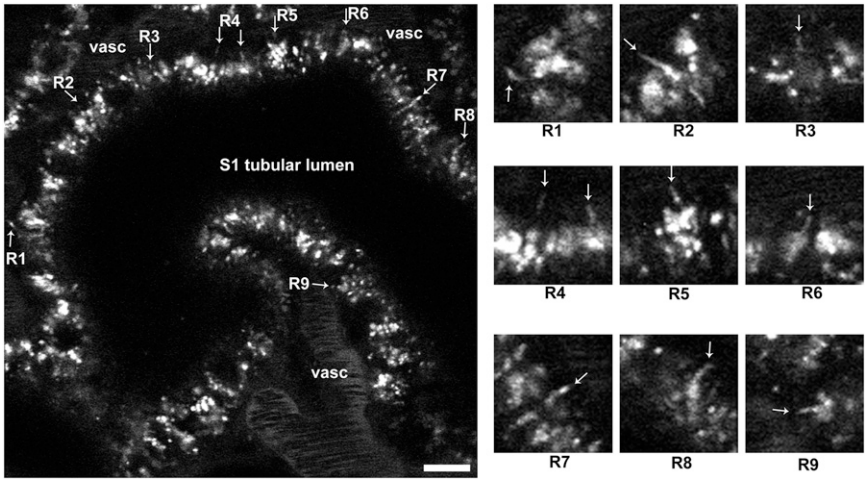

Figure 7. Transcytosis of RSA along the basal membrane occurs ubiquitously in the S1 proximal tubule cells of MW rats. An intravital cross-section of an S1 segment from a FMW rat shows accumulation and transcytosis of labeled albumin approximately 50 minutes after a bolus injection. The approximately 160-μm length spanning along the regions denoted (R1–R8) contained 150 detectable transcytotic events occurring at the basal membrane over a 3-minute, 40-second period. Assuming an average length of 14 μm per PTC in the X/Y orientation, this translates to approximately 54 transcytotic events (through tubular extension and vesicular trafficking) occurring at the basal membrane per cell/per minute. This value is probably an underestimation because the acquisition settings used to prevent saturation and blinding of the GaAsP detectors are incapable of detecting transcytotic structures whose fluorescent intensity falls below the minimum detection level. R1–R9 show the structure at either maximum extension in the case of tubular processes (R1, R2, R3, R4, R6, and R8) or vesicle at its closest proximity to the basal membrane (R5, R7, and R9). In Supplemental Movie 1, note the prolonged persistence of tubular extensions (such as R2), which are present for >90 seconds of this time-compressed 3-minute, 40-second movie. This is in stark contrast to the speed at which vesicles move (right of R5), approximately 1.1 μm/s. (Bar=10 μm.)

a sensitive nondescanned external detector allowed for maximal detection of low-intensity values found in Bowman's space for compounds with limited permeability. In this regard, Centonze and White previously delineated differences between descanned and nondescanned detectors.[30] Nondescanned detectors are more efficient in collecting emitted photons by avoiding the loss of signal due to the relatively longer light path from the specimen for a descanned mode and scattering introduced by the scanning mirrors and the other optical components during the descanning process. The absence of a pinhole further improves the sensitivity for the nondescanned mode because the pinhole aperture, which is present in the case of descanned mode (even though it is fully opened), can potentially block a portion of the emitted photons that originated from the focal point and scattered during the journey toward the detector. The extremely sensitive GaAsP detector[36] is an excellent choice for detecting the very low signal in the Bowman's space. With these detectors, less laser power is needed for imaging, resulting in less phototoxicity and subsequent tissue injury.

Our data also point out the potential flaws in using fluorescently labeled dextrans to model glomerular filtration dynamics. Careful characterization of the size distribution of the constituent polymers is required to avoid flawed interpretation of the data. In this study a time-dependent GSC_A was seen for a dextran with a wide distribution of small and large polymers, in which early GSC is falsely elevated by early clearance of the small polymers. These data were confirmed using standard gel filtration assays.

The potential effect of red blood cell crowding on the ability to accurately quantify plasma fluorescence was determined, and the present data refute previous claims. Because the reported speed of red blood cells within intraglomerular capillaries reported by Kang and colleagues[37] was 17.7 mm/sec and the scanning speed was 207 mm/sec, with a pixel dwell time of 2 microseconds and a pixel size of 0.414 μm, we felt it unlikely the movement of red blood cells would have any effect on plasma fluorescence intensity. Furthermore, the GSC value for fluorescein inulin reported previously was 1.050 ± 0.028 in our earlier study[19] and 1.03 ± 0.14 in Tanner and colleagues' study.[26] Underestimation of plasma intensity values at levels reported by Peti-Peterdi[23,25] would result in GSC values that are orders of magnitude greater than 1.0.

With use of our standardized imaging approach, a large effect of fasting was found on glomerular albumin permeability in both SMW and FMW rats. These data imply regulation of GSC_A and open new possibilities for the underlying mechanisms and clinical/pathologic importance. Previous work on the effects of feeding on single-nephron GFR will probably direct the initial investigations in this area.

Of note, the difference between the SMW and FMW rats under identical dietary conditions indicates a major difference in GSC_A, independent of diet, in those two strains of MW rats. Because previous micropuncture studies were done on fasting FMW rats (which we show here to have a relatively low GSC_A), the results between micropuncture GSC_A on FMW[38] and two-photon GSC_A on FMW rats (0.007) are less disparate than those seen in comparisons of GSC_A for fed SMW rats (0.030) and micropuncture on fasting FMW rats.[1,2,31,33] However, this value indicates a sizable difference in the amount of albumin filtered compared with that reported in micropuncture studies.

Increased glomerular permeability to albumin and a prolonged plasma half-life of albumin requires retrieval and recycling of filtered albumin.[18,19] Indeed, the consistent visualization of fluorescent albumin filtration, binding to and internalization across the membrane of proximal tubule cells, and subsequent trafficking to and fusion of intracellular vesicles and tubular

extensions with basal membranes provide additional proof for a dynamic and quantitatively significant retrieval pathway similar to those shown for FcRn-mediated trancystosis of IgG in cultured endothelial cells.[39] The occurrence of this phenomenon in conscious rats (as seen in Supplemental Figure 2) refutes previous assertions that this occurs only in rats maintained under poor physiologic condition.[24] These data extend our previous transmission electron microscopy data showing albumin-laden vesicles within PTCs and fusion of these vesicles with the basolateral membrane.[19] Taken together, our current study substantiates our previous findings and those from other investigators that attribute a greater role to the proximal tubules in maintaining albumin homeostasis under both physiologic and pathologic conditions. Because the final composition of albumin in the urine is affected by both glomerular filtration and proximal tubule reabsorption, both processes must be considered.

CONCISE METHODS

Animal Model

MW rats (both male and female) from a colony founded with breeders from Simonsen's Laboratory (Gilroy, CA) were used at ages no older than 16 weeks. Male MWF rats (males 10 weeks of age; n=5) were supplied by Harlan (Indianapolis, IN) or derived from a colony generously provided by Dr. Roland Blantz. Rats were also evaluated for strain and dietary condition differences in the glomerular filtration of albumin. Both strains were given water *ad libitum* during fed or overnight fasting conditions. Urinary albumin was quantified after 24-hour collection in metabolic cages, as described elsewhere.[28]

Fluorescent Albumin Synthesis

Rat serum albumin (fraction V, Sigma-Aldrich, St. Louis, MO) was conjugated to TR sulfonyl chloride as described elsewhere (Invitrogen, Carlsbad, CA) to give a stoichiometric ratio of 4:1 mol dye:albumin and was confirmed by determining the protein and fluorophore molar concentrations using absorbance measurements, as previously described.[19]

Dextrans

Commercially available 70-kD rhodamine B dextran was purchased from Invitrogen. The 69.7-kD fluorescein dextran was a gift from Dr. Wayne D. Comper. The 150-kD fluorescein and rhodamine dextran were provided by TdB Consultancy (Uppsala, Sweden). The 69.7-kD and 150-kD fluorescein dextrans were dialyzed against 0.9% saline using 50,000 and 100,000 molecular weight cutoff membranes, respectively (Spectrum Laboratories, Inc.); the 70-kDa rhodamine B dextran from Invitrogen was used without purification by dialysis.

Gel Filtration Chromatography

Toyopearl HW-55 resin (fractionation range, 1000–700,000; V_t=120 mL) was used to separate albumin and dextrans on the basis of molecular size. The column was equilibrated in PBS and calibrated using gel filtration molecular-weight markers (Sigma-Aldrich); the excluded (V_O) volume was determined with blue dextran. All samples were loaded in PBS 10% glycerol and column run at a flow rate of approximately 800 μl/min, and 1-mL fractions were collected and OD280 or fluorescence was measured to identify the elution profile for each molecule.

Two-Photon Microscopy

Imaging was conducted using an Olympus FV1000 microscope adapted for two-photon microscopy with high-sensitivity gallium arsenide nondescanned 12-bit detectors with animal preparations, as described elsewhere.[18] Additionally, the 60× water immersion objective with a numerical aperture of 1.2 was heated using a wrap-around objective heater (Warner Instruments, Hamden, CT). BP (via a femoral arterial line), body temperature, saline bath temperature in dish, and heart rate were measured using LabChart 6 (AD Instruments, Colorado Springs, CO). Body temperatures and the temperature of the saline in the coverslip dishes both fell between 36 and 38°C, and mean BP was 86.5±11.6 mmHg. Hydration status was maintained by intravenous infusion of a 0.9% saline solution at 1.5 mL/hr. Anesthesia in the SMW strain was induced using sodium pentobarbital (50 mg/mL; Ovation Pharmaceuticals, Deerfield, IL) at about 60 mg/kg. In the FMW rats, Inactin was used (130 mg/mL; Sigma-Aldrich) at approximately 160 mg/kg. A jugular venous line was used to introduce fluorescent conjugates.

Descanned and Nondescanned Detector Comparison

Vibratome sections from 4% paraformaldehyde-fixed rat kidneys were stained with a fluorescein-conjugated lectin from *L. culinaris* (Vector Laboratories, Burlingame, CA) and mounted in 1:1 glycerol: PBS w/2% 1,4-diazabicyclo[2.2.2]octane (Sigma) to retard photobleaching. A three-dimensional data set (shown in Figure 3) was first collected with internal (descanned) detectors, followed by external (nondescanned) multialkaline detectors, and finally on highly sensitive external (nondescanned) GaAs dectectors mounted on an Olympus Fluoview system using 10%, 10%, and 5% laser power for excitation, respectively. Data from the descanned detectors were collected first to assure that no bleaching occurred before imaging of this sample. The 12-bit images were quantified and graphed to show average fluorescence intensity per optical section as a function of depth.

Quantitative Process

The GSCs were determined using the steps outlined in Supplemental Figure 1. Briefly, images of the glomerulus were taken before infusion of fluorescent albumin or dextran conjugates to determine background levels within the capillary loops and Bowman's space. These background values were then subtracted from the corresponding intensity values to generate background-corrected values. The Bowman's space intensities were divided by the capillary loop plasma intensities to determine GSCs. Plasma intensity values for albumins and dextrans over time were determined by following the identical region within a plane of focus. Images were quantified using Metamorph, version 6.1 (Molecular Devices, Sunnyvale, CA). Graphs and mathematical summaries were generated using Microsoft Excel (Redmond, CA).

Transcytosis of Albumin

Male SMW rats (200 g) were given 2 mg of Alexa 568-RSA as an intravenous bolus injection *via* a jugular venous line. Imaging was

carried out 24 hours later using a BioRad MRC-1024 two-photon microscope; digitally zoomed movies were collected (at approximately 1 frame per second) to look for areas where transcytosis may be occurring. Photomultiplier sensitivity was adjusted to maximize detection of structures forming and projecting from bright intracellular structures containing filtered albumin, while minimizing optical "blooming" of these structures from oversaturation. As a result of these acquisition settings, the Alexa 568-RSA present in the microvasculature was not readily visible.

ACKNOWLEDGMENTS

Image collection and digital image analysis were conducted at the Indiana Center for Biological Microscopy. We thank Ken W. Dunn for critical review and suggestions.

This work was supported by National Institutes of Health (NIH) George M. O'Brien Award DK-61594, DK-076478, and a Department of Veterans Affairs merit review grant to B.A.M.

DISCLOSURES

None.

REFERENCES

1. Haraldsson B, Nyström J, Deen WM: Properties of the glomerular barrier and mechanisms of proteinuria. *Physiol Rev* 88: 451–487, 2008
2. Remuzzi A, Sangalli F, Fassi A, Remuzzi G: Albumin concentration in the Bowman's capsule: Multiphoton microscopy vs micropuncture technique. *Kidney Int* 72: 1410–1411, author reply 1411, 2007
3. Wang Y, Cai H, Cebotaru L, Hryciw DH, Weinman EJ, Donowitz M, Guggino SE, Guggino WB: ClC-5: Role in endocytosis in the proximal tubule. *Am J Physiol Renal Physiol* 289: F850–F862, 2005
4. Amsellem S, Gburek J, Hamard G, Nielsen R, Willnow TE, Devuyst O, Nexo E, Verroust PJ, Christensen EI, Kozyraki R: Cubilin is essential for albumin reabsorption in the renal proximal tubule. *J Am Soc Nephrol* 21: 1859–1867, 2010
5. Rangel-Filho A, Sharma M, Datta YH, Moreno C, Roman RJ, Iwamoto Y, Provoost AP, Lazar J, Jacob HJ: RF-2 gene modulates proteinuria and albuminuria independently of changes in glomerular permeability in the fawn-hooded hypertensive rat. *J Am Soc Nephrol* 16: 852–856, 2005
6. Sidaway JE, Davidson RG, McTaggart F, Orton TC, Scott RC, Smith GJ, Brunskill NJ: Inhibitors of 3-hydroxy-3-methylglutaryl-CoA reductase reduce receptor-mediated endocytosis in opossum kidney cells. *J Am Soc Nephrol* 15: 2258–2265, 2004
7. Verhulst A, D'Haese PC, De Broe ME: Inhibitors of HMG-CoA reductase reduce receptor-mediated endocytosis in human kidney proximal tubular cells. *J Am Soc Nephrol* 15: 2249–2257, 2004
8. Atthobari J, Brantsma AH, Gansevoort RT, Visser ST, Asselbergs FW, van Gilst WH, de Jong PE, de Jong-van den Berg LTW PREVEND study group: The effect of statins on urinary albumin excretion and glomerular filtration rate: Results from both a randomized clinical trial and an observational cohort study. *Nephrol Dial Transplant* 21: 3106–3114, 2006
9. Sarav M, Wang Y, Hack BK, Chang A, Jensen M, Bao L, Quigg RJ: Renal FcRn reclaims albumin but facilitates elimination of IgG. *J Am Soc Nephrol* 20: 1941–1952, 2009
10. Kim J, Bronson CL, Hayton WL, Radmacher MD, Roopenian DC, Robinson JM, Anderson CL: Albumin turnover: FcRn-mediated recycling saves as much albumin from degradation as the liver produces. *Am J Physiol Gastrointest Liver Physiol* 290: G352–G360, 2006
11. Carone FA, Ganote CE: D-serine nephrotoxicity. The nature of proteinuria, glucosuria, and aminoaciduria in acute tubular necrosis. *Arch Pathol* 99: 658–662, 1975
12. Yao B, Zhang MZ, Harris RC: A novel mouse model of AKI with targeted injury of proximal tubule cells. *J Am Soc Nephrol* 20: 733A, 2009
13. Menzel S, Kaldenbach M, Lanzmich R, Uhlig S, van Roeyen C, Rong S, Floege J, Moeller M: Transport of intact albumin from primary filtrate into the bloodstream in vivo. *J Am Soc Nephrol* 20: 62A, 2009
14. Gagliardini E, Conti S, Benigni A, Remuzzi G, Remuzzi A: Imaging of the porous ultrastructure of the glomerular epithelial filtration slit. *J Am Soc Nephrol* 21: 2081–2089, 2010
15. Dunn KW, Sandoval RM, Kelly KJ, Dagher PC, Tanner GA, Atkinson SJ, Bacallao RL, Molitoris BA: Functional studies of the kidney of living animals using multicolor two-photon microscopy. *Am J Physiol Cell Physiol* 283: C905–C916, 2002
16. Sandoval RM, Molitoris BA: Quantifying endocytosis in vivo using intravital two-photon microscopy. *Methods Mol Biol* 440: 389–402, 2008
17. Molitoris BA, Sandoval RM: Intravital multiphoton microscopy of dynamic renal processes. *Am J Physiol Renal Physiol* 288: F1084–F1089, 2005
18. Russo LM, Sandoval RM, Campos SB, Molitoris BA, Comper WD, Brown D: Impaired tubular uptake explains albuminuria in early diabetic nephropathy. *J Am Soc Nephrol* 20: 489–494, 2009
19. Russo LM, Sandoval RM, McKee M, Osicka TM, Collins AB, Brown D, Molitoris BA, Comper WD: The normal kidney filters nephrotic levels of albumin retrieved by proximal tubule cells: Retrieval is disrupted in nephrotic states. *Kidney Int* 71: 504–513, 2007
20. Rovira-Halbach G, Alt JM, Brunkhorst R, Frei U, Kühn K, Stolte H: Single nephron hyperfiltration and proteinuria in a newly selected rat strain with superficial glomeruli. *Ren Physiol* 9: 317–325, 1986
21. Tojo A, Endou H: Intrarenal handling of proteins in rats using fractional micropuncture technique. *Am J Physiol* 263: F601–F606, 1992
22. Eisenbach GM, Liew JB, Boylan JW, Manz N, Muir P: Effect of angiotensin on the filtration of protein in the rat kidney: A micropuncture study. *Kidney Int* 8: 80–87, 1975
23. Peti-Peterdi J, Sipos A: A high-powered view of the filtration barrier. *J Am Soc Nephrol* 21: 1835–1841, 2010
24. Tanner GA: Glomerular sieving coefficient of serum albumin in the rat: A two-photon microscopy study. *Am J Physiol Renal Physiol* 296: F1258–F1265, 2009
25. Peti-Peterdi J: Independent two-photon measurements of albumin GSC give low values. *Am J Physiol Renal Physiol* 296: F1255–F1257, 2009
26. Tanner GA, Rippe C, Shao Y, Evan AP, Williams JC Jr: Glomerular permeability to macromolecules in the Necturus kidney. *Am J Physiol Renal Physiol* 296: F1269–F1278, 2009
27. Corman B, Chami-Khazraji S, Schaeverbeke J, Michel JB: Effect of feeding on glomerular filtration rate and proteinuria in conscious aging rats. *Am J Physiol* 255: F250–F256, 1988
28. Schulz A, Hänsch J, Kuhn K, Schlesener M, Kossmehl P, Nyengaard JR, Wendt N, Huber M, Kreutz R: Nephron deficit is not required for progressive proteinuria development in the Munich Wistar Frömter rat. *Physiol Genomics* 35: 30–35, 2008
29. Licha K: Contrast agents for optical imaging. *Top Curr Chem* 222: 1–29, 2002
30. Centonze VE, White JG: Multiphoton excitation provides optical sections from deeper within scattering specimens than confocal imaging. *Biophys J* 75: 2015–2024, 1998
31. Comper WD, Russo LM: The glomerular filter: an imperfect barrier is required for perfect renal function. *Curr Opin Nephrol Hypertens* 18: 336–342, 2009
32. Hallan SI, Ritz E, Lydersen S, Romundstad S, Kvenild K, Orth SR: Combining GFR and albuminuria to classify CKD improves prediction of ESRD. *J Am Soc Nephrol* 20: 1069–1077, 2009

33. Nielsen R, Christensen EI: Proteinuria and events beyond the slit. *Pediatr Nephrol* 25: 813–822, 2010
34. Molitoris BA: Yet another advance in understanding albuminuria? *J Am Soc Nephrol* 21: 2013–2015, 2010
35. Gekle M: Renal tubule albumin transport. *Annu Rev Physiol* 67: 573–594, 2005
36. Zipfel WR, Williams RM, Webb WW: Nonlinear magic: Multiphoton microscopy in the biosciences. *Nat Biotechnol* 21: 1369–1377, 2003
37. Kang JJ, Toma I, Sipos A, McCulloch F, Peti-Peterdi J: Quantitative imaging of basic functions in renal (patho)physiology. *Am J Physiol Renal Physiol* 291: F495–F502, 2006
38. Gekle M: Renal albumin handling: a look at the dark side of the filter. *Kidney Int* 71: 479–481, 2007
39. Prabhat P, Gan Z, Chao J, Ram S, Vaccaro C, Gibbons S, Ober RJ, Ward ES: Elucidation of intracellular recycling pathways leading to exocytosis of the Fc receptor, FcRn, by using multifocal plane microscopy. *Proc Natl Acad Sci U S A* 104: 5889–5894, 2007

See related editorial, "Illuminating the Glomerular Filtration Barrier, Two Photons at a Time," on pages 373–375.

This article contains supplemental material online at http://jasn.asnjournals.org/lookup/suppl/doi:10.1681/ASN.2011070666/-/DCSupplemental.